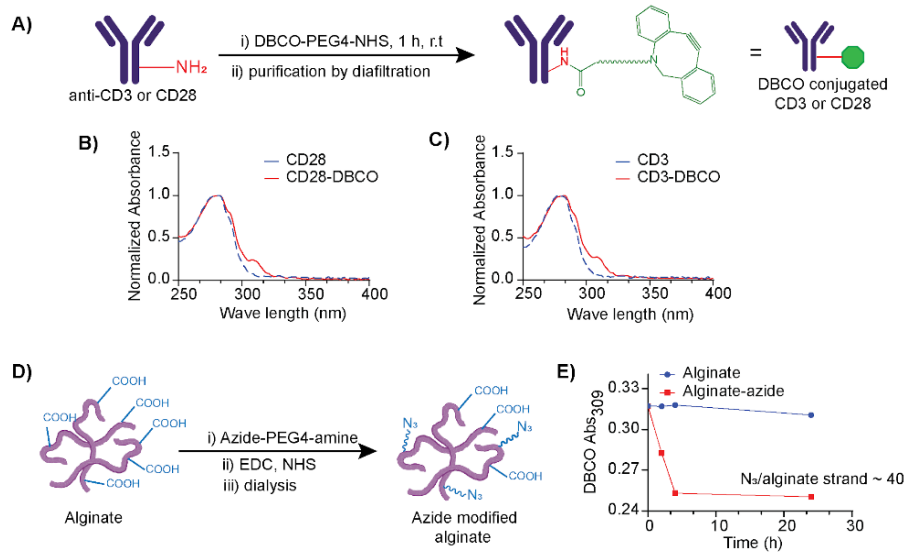
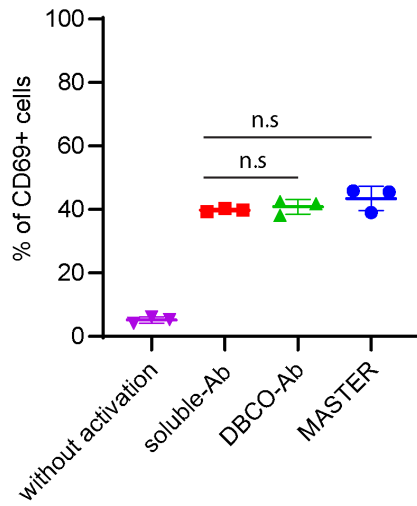


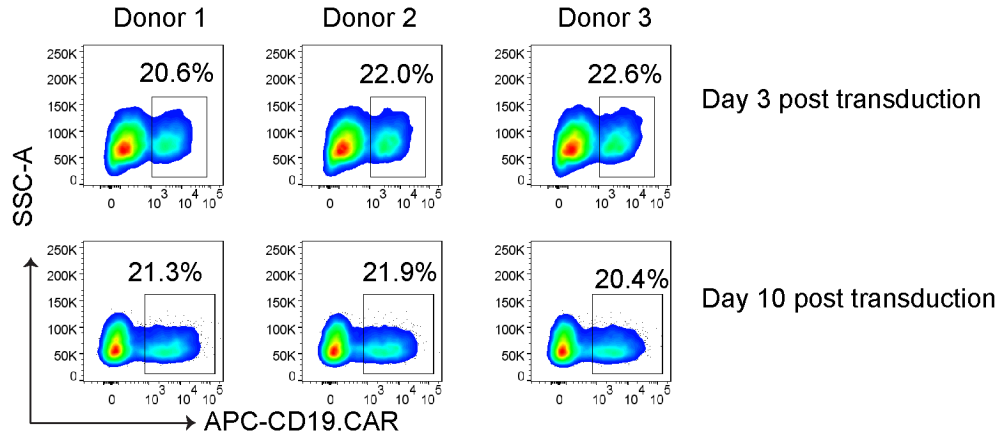
Supplementary Figures:



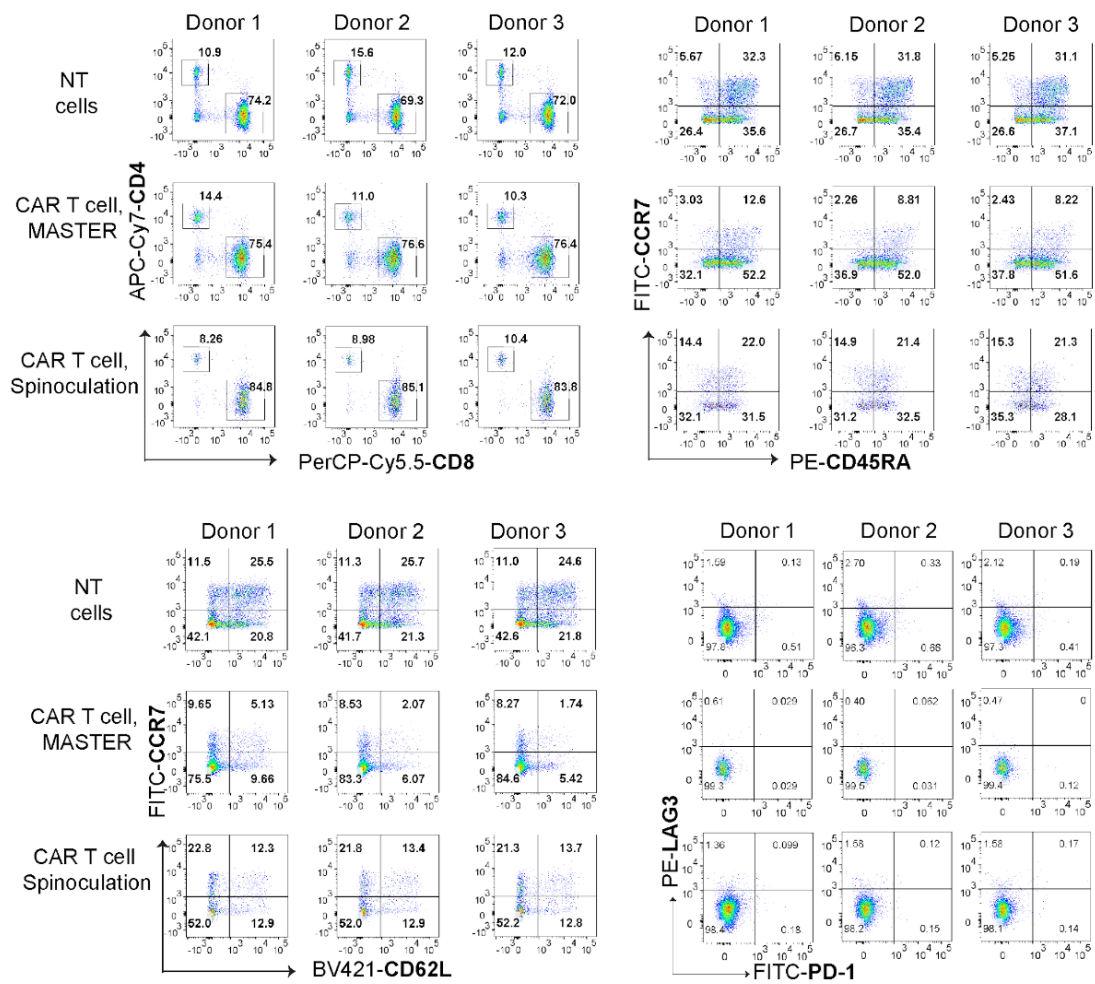
Supplementary Figure 1: Synthesis of MASTER components. A) schematic for conjugation of anti-CD3 and anti-CD28 antibodies with dibenzocyclooctyne (DBCO). B) UV-absorption spectra of DBCO-conjugated ant-CD28 antibody showing distinct absorption peak of DBCO at 309 nm. C) UV-absorption spectra of DBCO-conjugated anti-CD3 antibody showing distinct absorption peak of DBCO at 309 nm. D) Synthetic scheme for azide-modified alginate E) Quantification of number of azides per alginate strand



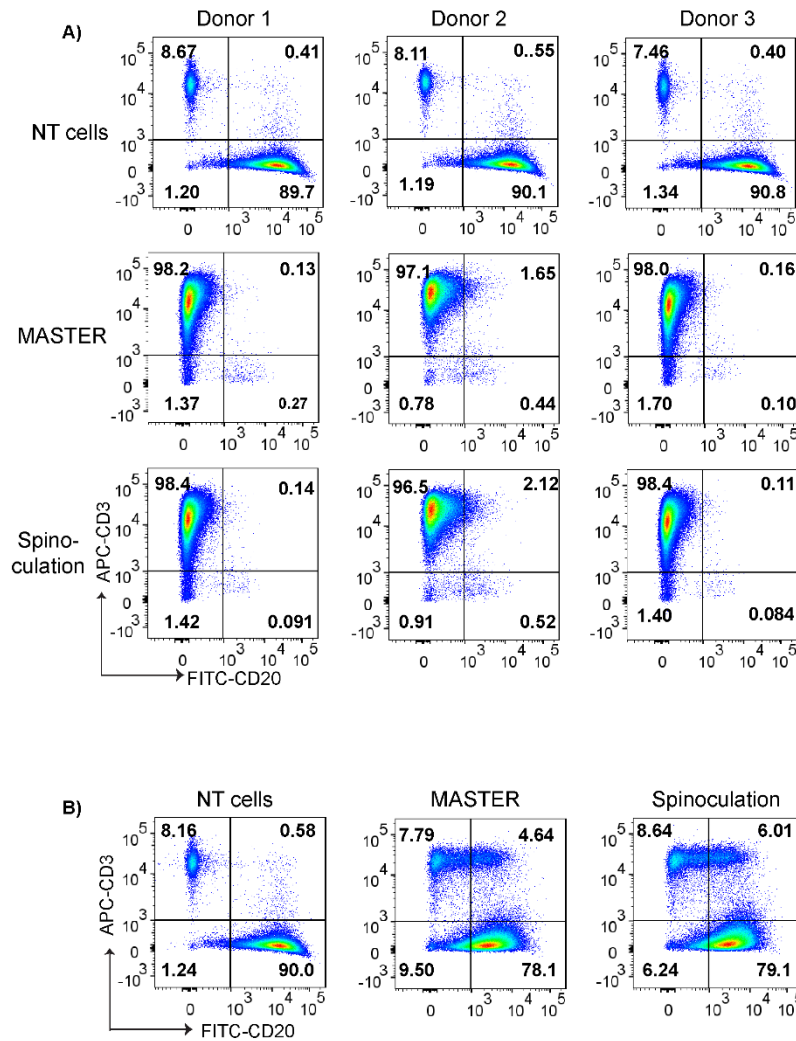
Supplementary Figure 2: CD69 expression in T cells seeded on plates with soluble antibodies, DBCO-conjugated antibodies and on MASTER (n.s = non-significant, unpaired t test). Equivalent amounts of antibodies were used for each group. Data represent mean \pm SD of three biologically independent samples.



Supplementary Figure 3: FACS analysis of T cells on Day 3 and Day 10 post-transduction. T cells from three different donors were transduced with CD19.CAR encoding gamma retrovirus on MASTER and analyzed for CAR expression by flow cytometry.



Supplementary Figure 4: Phenotypic characterization of produced CAR-T cells. CD4/CD8 (A), CD45RA/CCR7 (B), CD62L/CCR7 (C) and PD-1/LAG3 (D) expression in CAR-T cells from 3 different donors generated by MASTER or by spinoculation. The analyses were performed on CAR-expressing cells except for non-transduced (NT) cells.



Supplementary Figure 5: CAR-T cells generated by MASTER-mediated transduction show toxicity against CD19⁺ tumor cells (A) but not against CD19⁻ U937 cells (B). CD19⁺ tumor cells or CD19⁻ U937 cells were co-cultured with control non-transduced cells (NT cells) or CD19.CAR-T cells generated by MASTER mediated transduction or by spinoculation at 1:5 E:T ratio and analyzed by FACS on day 5 of co-culture.

Microscopic Observation from Blinded Veterinary Pathologist:

Key:

M1-M3: untreated controls

M4-M6: MASTER scaffolds

M7-M9: MASTER scaffolds seeded with mouse PBMCs and GFP-encoding retrovirus.

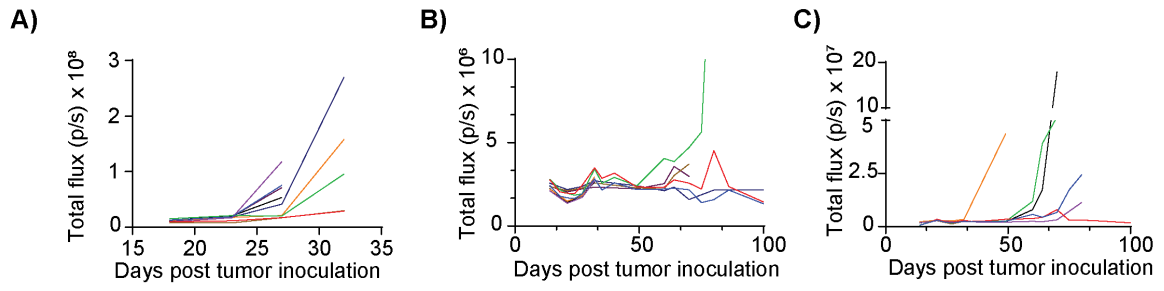
Images of heart, liver, lung, kidney, spleen and skin were examined from 9 mice. Images of some replicate sections of spleen and skin were included to optimize viewable sections of each tissue.

No noteworthy changes were observed in M1 or M2; all tissues were within normal limits. The only observation in M3 was a mild focal strain-related finding in the lung. This is common in C57BL6 mice and in some other strains and would not be related to experimental treatment.

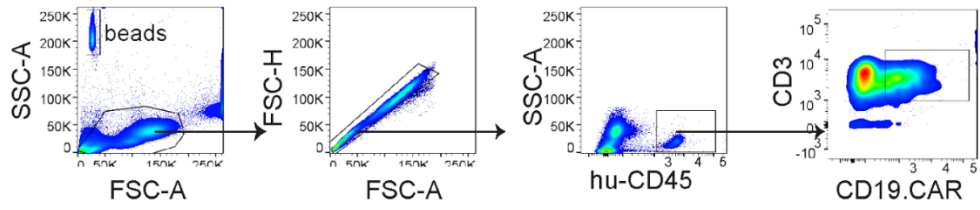
Mice M4 - M9 all had subcutaneous pockets in the skin sections. These were bounded by thin fibrous capsules with a sparse macrophage component. The space of the pockets contained a faint meshwork of material admixed with a very few macrophages, and usually a small island of somewhat darker (more dense-appearing) material. Surrounding dermal connective tissue generally contained a slight infiltration of cells considered to be macrophages and presumably fibroblasts. No evidence of toxicity was observed in skin-associated skeletal muscle, adnexa or epidermis. No evidence of toxicity or other deleterious effect was observed in any of the other tissues examined.

Sample	RBC (M/ μ L)	WBC (K/ μ L)	Neutrophil (/ μ L)	Monocyte (/ μ L)	Eosinophil (/ μ L)	Basophil	Lymphocyte (%)	HCT (%)	Absolute reticulocyte (K/ μ L)	HGB (g/dL)	MCV (fL)	MCH (pg)	MCHC (g/dL)	Platelet Count (K/ μ L)	Poikilocytosis	Polychromasia	Heinz bodies	Metamyelocyte (%)	Myelocyte	Promyelocyte (%)	Unclassified (%)
Untreated control	9.89 \pm 0.5	7.8 \pm 1.6	333.67 \pm 24.4	352 \pm 95.8	120 \pm 57.4	7.66 \pm 6.8	89.43 \pm 1.6	45.8 \pm 1.4	317.3 \pm 46.54	14.2 \pm 0.9	46.3 \pm 1.15	14.4 \pm 0.17	30.96 \pm 1.07	966 \pm 65.19	none seen	slight	None seen	None seen	None seen	None seen	None seen
MASTER	10.09 \pm 0.2	6.5 \pm 0.4	331.33 \pm 19.5	280 \pm 56.8	131.3 \pm 57.7	10.33 \pm 9.6	88.4 \pm 1.9	47 \pm 1.63	360.6 \pm 33.29	14.3 \pm 0.3	47 \pm 1	14.36 \pm 0.05	30.6 \pm 0.34	945 \pm 39.71	none seen	Moderate	None seen	None seen	None seen	None seen	None seen
MASTER + cells + virus	9.86 \pm 0.5	6.06 \pm 1.07	315.67 \pm 47.1	219 \pm 54.4	199.3 \pm 88.7	6 \pm 5.5	87.6 \pm 1.6	45.8 \pm 0.7	335 \pm 44.23	14.03 \pm 0.5	46.6 \pm 1.5	14.23 \pm 0.2	30.6 \pm 0.66	967 \pm 144.8	none seen	Moderate	None seen	None seen	None seen	None seen	None seen

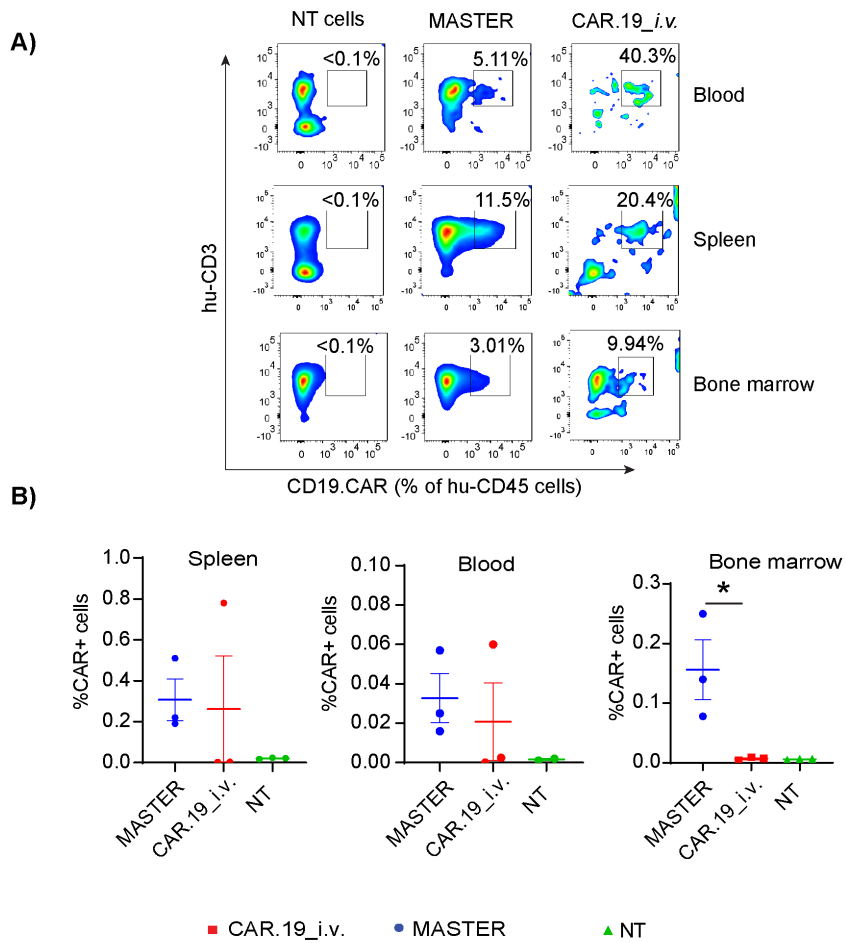
Supplementary Figure 6: Biocompatibility of MASTER and its components as revealed by biochemical analysis of mouse blood. MASTER and MASTER + mouse PBMCs + GFP encoded gamma retrovirus were implanted in the subcutaneous space of C57Bl6/J immunocompetent mice (n=3). Untreated mice were kept as controls.



Supplementary Figure 7: Individual tumor growth curves of mice treated with NT cells (A), MASTER (B) or i.v. infused with CAR T cells (C). Each line represents one animal. Data are shown for nine mice per treatment condition.



Supplementary Figure 8: Gating strategy for detection of CAR+ cells in blood, bone marrow or spleen.



Supplementary Figure 9: A) Representative flow cytometry plots showing human CD45+CD3+CAR+ cells isolated from blood, bone marrow and spleen of mice (n=3) at day 32 post tumor cell inoculation. B) % of human CD3+CAR+ of total cells in in blood, bone marrow and spleen of mice euthanized at day 32 after tumor cell inoculation, as determined by flow cytometry. Data in f-h represent mean \pm SEM of three experimental replicates